Experimental extraction of donor-driven spin relaxation in *n*-type nondegenerate germanium

M. Yamada,[1,2,*] T. Ueno,[3] T. Naito,[3] K. Sawano,[4] and K. Hamaya[2,†]

[1]*PRESTO, Japan Science and Technology Agency, 4-1-8 Honcho, Kawaguchi, Saitama 332-0012, Japan*

[2]*Center for Spintronics Research Network, Graduate School of Engineering Science, Osaka University, 1-3 Machikaneyama, Toyonaka 560-8531, Japan*

[3]*Department of Systems Innovation, Graduate School of Engineering Science, Osaka University, 1-3 Machikaneyama, Toyonaka, Osaka 560-8531, Japan*

[4]*Advanced Research Laboratories, Tokyo City University, 8-15-1 Todoroki, Tokyo 158-0082, Japan*

(Received 23 July 2021; accepted 14 August 2021; published 1 September 2021)

Using pure spin current transport measurements in lateral spin-valve devices, we study the spin relaxation in an *n*-type nondegenerate Ge layer, which is moderately doped Ge (P: $\sim 10^{18}$ cm^{-3}). The obtained spin diffusion length (λ_{Ge}) of the nondegenerate Ge is two to three times greater than that of heavily doped degenerate Ge (P: $\sim 10^{19}$ cm^{-3}) in the temperature range from 8 to 100 K. We find that the electron spin lifetime (τ) for the nondegenerate Ge is monotonically increased with decreasing temperature (T). The increase in τ at temperatures less than 50 K can be interpreted in terms of the donor-driven spin relaxation mechanism including the $1/\sqrt{T}$ behavior in multivalley semiconductors, proposed by Song *et al.* [Y. Song, O. Chalaev, and H. Dery, Phys. Rev. Lett. **113**, 167201 (2014)]. We note that it is important for the τ of the moderately doped nondegenerate Ge to partly consider the T-independent component of spin relaxation in addition to the $1/\sqrt{T}$ component.

DOI: 10.1103/PhysRevB.104.115301

I. INTRODUCTION

Spin transport phenomena in semiconductors have been explored to develop methods for controlling spin degrees of freedom for semiconductor device structures [1–5]. For III-V semiconductors having broken lattice inversion symmetry, the D'yakonov–Perel' (DP) spin relaxation mechanisms have been revealed experimentally [1,6] because their spin states can be determined using well-established optical [7–9] and electrical [3,10] methods. Recently, the temperature dependence of the spin lifetime (τ) for GaAs was investigated using electrical methods at temperatures as high as room temperature [11]. However, the literature contains few reports on the room-temperature spin transport in GaAs [11–13] because the DP spin relaxation in GaAs leads to the very short τ less than 100 picoseconds at room temperature. In addition, the report on the doping concentration dependence of the τ for GaAs has been still limited at temperatures less than 5 K [8].

For group IV semiconductors such as Si and Ge, on the other hand, relatively long τ values can be obtained even at room temperature because of inversion symmetry in their crystal structure and their relatively weak spin-orbit interaction [14–19]. The spin-flip mechanism in Si and Ge has been discussed on the basis of the Elliott-Yafet (EY) mechanism induced by the spin-orbit interaction of host materials [20–23]. However, a contradiction created by the strong dependence of electron spin relaxation on the species of donor atoms in Si was also pointed out a long time ago [24]. To explain the difference in τ for different donor species, Song *et al.* predicted that intervalley spin-flip scattering via the central core potential of impurities would be dominant in Si and Ge with a multivalley-structured conduction band [25]. In this theory, the difference in the energy split induced by spin-orbit coupling of the donor atoms leads to variations that depend on the dopant species. Recently, for heavily doped degenerate Si and Ge, we experimentally clarified the presence of donor-induced intervalley scattering of spins through investigations of the impurity-concentration dependence [26] and temperature (T) dependence [17,27,28] of the τ.

For simplification, we focus on Ge as one of the group IV multivalley semiconductors. The proposed donor-induced intervalley spin-flip scattering rate ($\frac{1}{\tau_{\mathrm{donor}}}$) for Ge can be expressed as [25]

$$\frac{1}{\tau_{\mathrm{donor}}} \approx \frac{4\pi N_{\mathrm{d}} m_{\mathrm{e}} a_{\mathrm{B}}^6}{27\hbar^4}\sqrt{2m_{\mathrm{e}}\epsilon_{\mathrm{k}}}\,\Delta_{\mathrm{so}}^2. \tag{1}$$

Here, N_{d} is the donor concentration, a_{B} is the Bohr radius in Ge, m_{e} is the electron effective mass in Ge, ϵ_{k} is the conduction electron energy, and Δ_{so} is the spin–orbit-coupling-induced splitting of the triply degenerate $1s$ (T_2) donor state in Ge. When the thermal energy ($k_{\mathrm{B}}T$) is greater than the Fermi energy (ϵ_{F}), i.e., $\epsilon_{\mathrm{F}} \leqslant k_{\mathrm{B}}T$, where k_{B} is Boltzmann's constant, we can assign $k_{\mathrm{B}}T$ to ϵ_{k} in Eq. (1); hence, τ_{donor} is proportional to $1/\sqrt{T}$. For heavily doped Ge (P: $\sim 10^{19}$ cm^{-3}), Dushenko *et al.* reported that the T dependence of τ in the T range from 130 to 297 K exhibits the $1/\sqrt{T}$ behavior on the basis of donor-induced intervalley scattering [29]. However, in the heavily doped Ge, ϵ_{F} can be generally assigned as ϵ_{k} because the position of the ϵ_{F} is much larger than $k_{\mathrm{B}}T$ ($\epsilon_{\mathrm{F}} \geqslant k_{\mathrm{B}}T$). That is, the donor-induced spin

*michihiro@ee.es.osaka-u.ac.jp
†hamaya@ee.es.osaka-u.ac.jp

scattering term in Eq. (1) is almost constant in the T range from 130 to 297 K. On the other hand, Fujita *et al.* argued that the T-independent τ at low temperatures [27] and the weak T dependence of τ at high temperatures ($T \geqslant 130$ K) were attributable to a dominant component of phonon-induced spin-flip scattering in addition to the influence of the impurity scattering [28]. Therefore, as an evident influence of the impurity on the spin relaxation, the appearance of the $1/\sqrt{T}$ behavior of τ remains unclear in the field of spin relaxation mechanism of the group IV multivalley semiconductors such as Si and Ge.

In the present study, we experimentally extract the $1/\sqrt{T}$ behavior of τ by investigating pure spin current transport in moderately doped Ge (P: $\sim 10^{18}$ cm^{-3}) unlike heavily doped Ge (P: $\sim 10^{19}$ cm^{-3}) shown in previous works [27–29]. Here, because the moderately doped Ge clearly shows electrical properties derived from nondegenerate semiconductors, we call it nondegenerate Ge. The spin diffusion length in the nondegenerate Ge is two to three times greater than that in the heavily doped degenerate Ge (P: $\sim 10^{19}$ cm^{-3}) in Ref. [27] in the temperature range from 8 to 100 K. For the nondegenerate Ge, we observe a monotonic increase in τ with decreasing T from 100 to 8 K. Although the nondegenerate Ge studied here still has relatively large ϵ_F compared to $k_B T$ at low temperatures, the monotonic increase in τ at temperatures less than 50 K can be interpreted in terms of the donor-driven spin relaxation mechanism including the $1/\sqrt{T}$ behavior in multivalley semiconductors, proposed by Song *et al.* [25]. We note that it is important for the τ of the moderately doped nondegenerate Ge to partly consider the T-independent component of spin relaxation in addition to the $1/\sqrt{T}$ component.

II. FABRICATION AND CHARACTERIZATION OF NONDEGENERATE GE

To explore the spin transport properties in nondegenerate Ge, we fabricated and characterized a moderately doped n-Ge channel layer. First, we grew an undoped Ge buffer layer, consisting of a 28-nm-thick Ge layer grown at 350° C (LT-Ge) and a 70-nm-thick Ge layer grown at 700° C (HT-Ge), on a high-resistivity Si(111) substrate ($\sim$1000 Ω · cm) using a two-step growth technique with molecular beam epitaxy (MBE) [30]. On the undoped Ge buffer layer, a P-doped Ge layer (doping concentration $\sim 10^{18}$ cm^{-3}) with a thickness of 140 nm was grown at 350° C, where the growth temperature was lowered to efficiently incorporate the P atoms into Ge. The electrical properties of the P-doped Ge layer were determined using longitudinal resistance (V_{xx}/I) and Hall voltage (V_{xy}) of the Hall-bar device as illustrated in Fig. 1(a).

Figures 1(b) to 1(d) show the temperature dependence of resistivity (ρ_{Ge}), carrier density (n), and electron mobility (μ) for the moderately doped Ge (red plots), together with the data for heavily doped Ge (blue plots) in Ref. [27]. With decreasing temperature from 300 to 8 K, the ρ_{Ge} of the moderately doped channel increases from 13.3 to 21.2 mΩ · cm, indicating nondegenerate semiconductor behavior, unlike that of the heavily doped Ge. The n and μ in the moderately doped Ge layer are estimated to be 1.1×10^{18} cm^{-3} and 440 cm^2/(V · s) at 300 K, respectively, and, in the entire T range, the n is nearly one order of magnitude smaller than that of the heavily doped Ge.

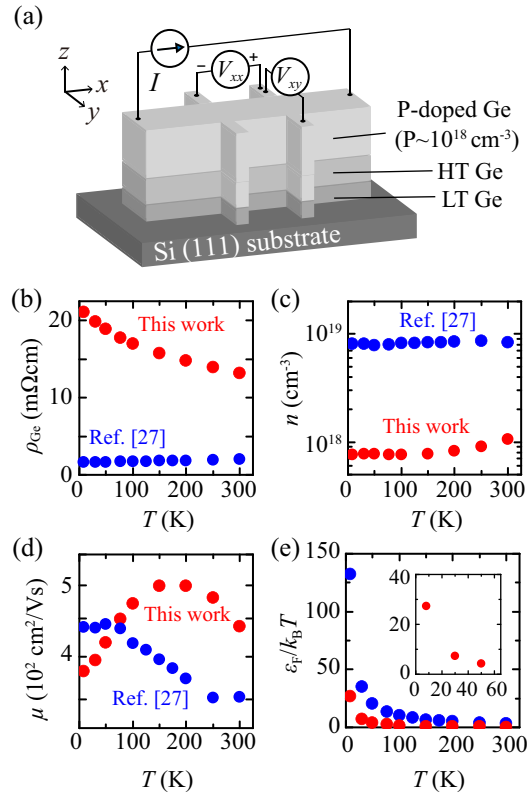

FIG. 1. (a) Schematic of a Hall-bar device with a moderately doped Ge (P: $\sim 10^{18}$ cm^{-3}) layer. The temperature dependence of (b) ρ_{Ge}, (c) n, (d) μ, and (e) ϵ_F/k_BT for the moderately doped Ge layer (red), together with that for the heavily doped Ge (P: $\sim 10^{19}$ cm^{-3}) (blue) reported elsewhere [27].

The μ in the moderately doped Ge layer is lower than that reported in the literature for bulk Ge with a similar doping level [31] because the defects in the P-doped Ge layer are introduced during the low-temperature growth. In this study, since the moderately doped Ge clearly shows nondegenerate semiconductor behavior in $\rho_{Ge} - T$ [Fig. 1(b)] and $n - T$ [Fig. 1(c)] curves, we call it nondegenerate Ge.

To consider the spin relaxation related to Eq. (1) later, the value of ϵ_F/k_BT for the nondegenerate Ge is calculated in Fig. 1(e), also together with the data for the heavily doped (degenerate) Ge in Ref. [27]. Here the ϵ_F can roughly be regarded as $\frac{\hbar^2}{2m_e}(3\pi^2 n)^{2/3}$. As expected, although the value of ϵ_F/k_BT for the nondegenerate Ge is smaller than that for the degenerate Ge, the ϵ_F is still greater than the k_BT for the nondegenerate Ge below 50 K, as shown in inset of Fig. 1(e). Thus, it should be noted that the nondegenerate Ge in this study is not completely satisfied with the ideal condition of $\epsilon_F \leqslant k_BT$, leading to the $1/\sqrt{T}$ component in Eq. (1), at low temperatures.

III. RESULTS AND DISCUSSION

Lateral spin-valve (LSV) devices with a nondegenerate Ge channel layer were fabricated to explore the spin transport properties, as illustrated in Fig. 2(a). For the tunnel conduction from the ferromagnet (FM) to the Ge spin transport layer

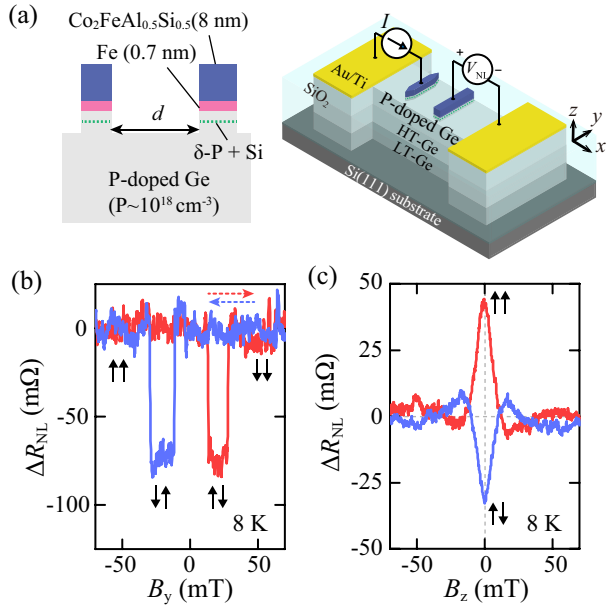

FIG. 2. (a) Schematic of a fabricated CFAS/Fe/Ge-based LSV device. A cross section of the CFAS/Fe/Ge structure is also shown on the left. (b) Nonlocal magnetoresistance and (c) nonlocal Hanle effect curves for an LSV with $d = 2.0$ μm, measured at $I = -0.5$ mA at 8 K.

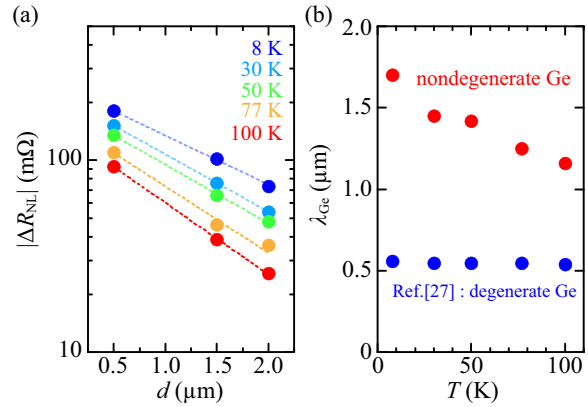

FIG. 3. (a) The d dependence of $|\Delta R_{NL}|$ for the LSV with nondegenerate Ge at various temperatures. The dashed lines fitted to Eq. (2). (b) The T dependence of λ_{Ge} for the LSV with nondegenerate Ge (red), together with that for the LSV with degenerate Ge (blue) reported elsewhere [27].

through the Schottky barrier, a P δ-doped Ge layer with an ultrathin Si insertion layer was grown on the moderately doped Ge layer at 400° C [32]. To obtain large spin signals, we used a double FM layer structure consisting of $Co_2FeAl_{0.5}Si_{0.5}$ (CFAS) (8 nm)/Fe (0.7 nm) grown by low-temperature MBE, where the 0.7-nm-thick Fe layer prevents the outdiffusion of Ge into the CFAS layer, resulting in an atomically controlled CFAS/Fe/n-Ge interface [33]. Spin injector and detector contacts with areas of 0.4×10 μm^2 and 0.5×10 μm^2, respectively, were fabricated on the FM and δ-doped Ge layers using electron beam lithography and Ar^+-ion milling, where the edge-to-edge distance (d) between the FM contacts was varied from 0.5 to 2.0 μm [see left schematic diagram of Fig. 2(a)]. Four-terminal nonlocal (NL) voltages (ΔV_{NL}) were measured in the terminal configuration shown in the right of Fig. 2(a) under in-plane (B_y) or out-of-plane (B_z) applied magnetic fields. Figures 2(b) and 2(c) show representative NL magnetoresistance and Hanle curves recorded at $I = -0.5$ mA at 8 K for an LSV device with $d = 2.0$ μm. A clear NL magnetoresistance change ($\Delta R_{NL} = \Delta V_{NL}/I \sim 70$ mΩ) that depends on the magnetization states of the FM contacts is observed after long-distance spin transport in the nondegenerate Ge. NL Hanle effect curves are also observed for both parallel and antiparallel magnetization configurations, as shown in Fig. 2(c). These results evidently show that large spin accumulation and electron spin transport were achieved even in nondegenerate Ge.

In the present study, the spin lifetime in Ge (τ_{Ge}) is estimated on the basis of the relationship $\lambda = \sqrt{D\tau}$, where D is the diffusion constant. First, we focus on the spin diffusion length of Ge (λ_{Ge}). To determine the λ_{Ge} in nondegenerate n-Ge, we measured ΔR_{NL} for the LSV devices with various d. Figure 3(a) shows the d dependence of the magnitude of ΔR_{NL} ($|\Delta R_{NL}|$) at various temperatures. With increasing d, $|\Delta R_{NL}|$ was found to decay exponentially at all of the investigated temperatures. In general, the decay of $|\Delta R_{NL}|$ with increasing d can be expressed by the equation [34–37]

$$|\Delta R_{NL}| = \frac{|P_{inj}||P_{det}|\rho_{Ge}\lambda_{Ge}}{S}\exp\left(-\frac{d}{\lambda_{Ge}}\right), \qquad (2)$$

where P_{inj} and P_{det} are the spin injection efficiency and the detection efficiency, respectively, and S is the cross section (1.68 μm^2) of the n-Ge channel layer. The λ_{Ge} can be estimated by fitting the decay of $|\Delta R_{NL}|$ with Eq. (2) in the T range from 8 to 100 K, as shown in Fig. 3(a). The T dependence of λ_{Ge} is presented in Fig. 3(b), together with our previously reported λ_{Ge} for LSVs with a degenerate Ge layer [27]. The value of λ_{Ge} for the nondegenerate Ge is 1.70 μm at 8 K, which is two to three times greater than that for the degenerate Ge. Notably, the value of λ_{Ge} for the nondegenerate Ge decreases rapidly from 1.70 to 1.16 μm with increasing T, while that for the degenerate Ge is independent of T in the range from 8 to 100 K [27,28].

Using the determined λ_{Ge}, we estimate τ_{Ge} from the relation of $\lambda_{Ge} = \sqrt{D\tau_{Ge}}$. Here we calculated the D values from the n and μ measured on the basis of the results in Fig. 1 and Eq. (4) in Ref. [38]. In Fig. 4, τ_{Ge} is plotted as a function of T, together with other data shown in previous works [23,27,39], and the inset shows the T dependence of the calculated D. Unlike the degenerate Ge (blue) in Ref. [27], the τ_{Ge} for the nondegenerate Ge (red) increases monotonically with decreasing T, reaching 6.0 ns at 8 K, which is one order of magnitude longer than the τ_{Ge} in the degenerate Ge in Ref. [27]. Furthermore, the value of τ_{Ge} is also much longer than those in other nondegenerate Ge reported in Refs. [23,39]. In the following, we discuss the difference in the situation among Refs. [23,39] and this study. In Ref. [23], the authors used four-terminal NL Hanle-effect measurements to obtain the value of τ_{Ge}. It was mentioned that the degenerate Ge layer ($\sim 2 \times 10^{19}$ cm^{-3}) for tunnel conduction between

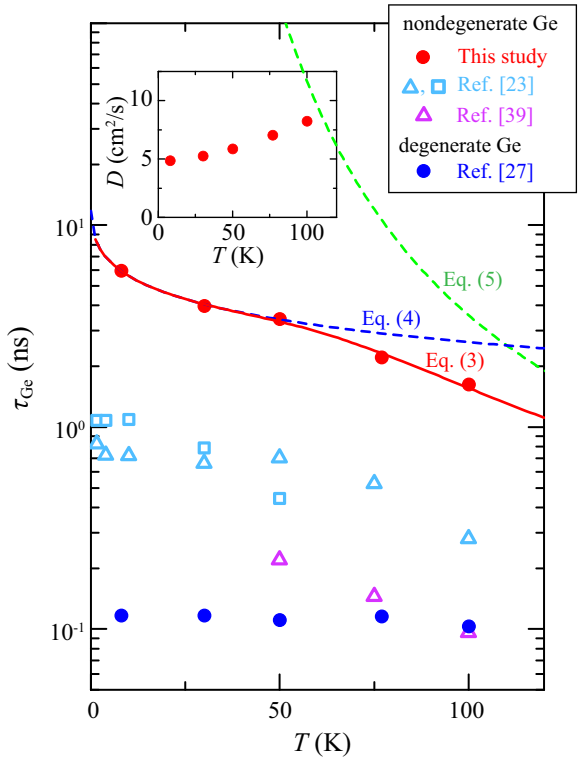

FIG. 4. T dependence of τ_{Ge} for the LSV with nondegenerate Ge (red), together with those for an LSV with degenerate Ge (blue) reported in Ref. [27] and an LSV with nondegenerate Ge reported in Ref. [23] (cyan) and in Ref. [39] (purple). The solid and dashed curves indicate the results of fitting to Eqs. (3), (4), and (5). The inset shows a plot of D versus T for the nondegenerate Ge.

the FM and nondegenerate Ge ($\sim 10^{16}$ cm^{-3}) remained in the channel region. Because of the presence of the degenerate Ge layer in the spin transport channel, the electron spins mainly conducted in the degenerate layer, leading to the decrease in the τ_{Ge} due to the impurity-induced spin relaxation, as the authors discussed. In Ref. [39], the spin transport channel was a nondegenerate Ge ($\sim 5 \times 10^{17}$ cm^{-3}) in the devices, the authors used three-terminal Hanle-effect measurements to obtain the value of τ_{Ge}. In the used devices, because there was an Sb δ-doped Ge layer at the FM/Ge interfaces, the influence of the impurity-induced spin relaxation by the Sb δ-doping layer was enhanced, where the impurity-induced spin relaxation derived from Sb was stronger than that from P [40]. In this study, on the contrary, the P δ-doped Ge layer are removed completely from the channel region during fabrication of the LSV devices [see Fig. 2(a)]; thus, the spin scattering in the P δ-doped Ge layers can be neglected in the four-terminal NL spin transport measurements [18,26,28]. That is, the transport properties in Figs. 3 and 4 estimated from relatively large spin signals in reliable LSV devices are attributed to nondegenerate Ge. Therefore, the τ_{Ge} longer than those in previous reports [23,39] can be regarded as appropriate data for the nondegenerate Ge.

To elucidate the monotonic T dependence of τ_{Ge} in Fig. 4, we analyze the data on the basis of recent theories [25,41]. According to Matthiessen's rule, if we consider the impurity- and phonon-induced inter and intravalley spin-flip scatterings in Ge, then the spin scattering rate ($\frac{1}{\tau_{Ge}}$) can be expressed as

$$\frac{1}{\tau_{Ge}} = \frac{1}{\tau_{imp}} + \frac{1}{\tau_{phon}^{inter}} + \frac{1}{\tau_{phon}^{intra}}, \tag{3}$$

where τ_{imp}, τ_{phon}^{inter}, and τ_{phon}^{intra} are spin lifetimes due to the impurity-induced (donor-driven) [25] and phonon-induced [41] inter and intravalley spin-flip scatterings, respectively. In this case, the phonon-induced intravalley spin-flip scattering ($\frac{1}{\tau_{phon}^{intra}}$) is negligibly small [17,26–28,41]. For the nondegenerate Ge at low temperatures, we assume that the $\frac{1}{\tau_{imp}}$ term can be regarded as the modified Eq. (1) [25,26]:

$$\frac{1}{\tau_{imp}} \approx \frac{1}{\tau_{imp0}} + \frac{4\pi n m_e a_B^6}{27\hbar^4}\sqrt{2m_e k_B T}\,\Delta_{so}^2. \tag{4}$$

Here, τ_{imp0} is a T-independent term under the condition of $\epsilon_F \gg k_B T$. For the second term in Eq. (4), we assigned $k_B T$ to $\epsilon_{\mathbf{k}}$ in Eq. (1) and assumed that $a_B = 6.45$ nm [42] and $m_e = 0.16 m_0$ [43]. As described in Eq. (4), the $\frac{1}{\tau_{imp}}$ term is related to $1/\sqrt{T}$. In the T range from 8 to 100 K, n is approximately constant and regarded as $\sim 7.7 \times 10^{17}$ cm^{-3}. The τ_{phon}^{inter} term can be expressed as [41]

$$\frac{1}{\tau_{phon}^{inter}} = \frac{4}{3}\left(\frac{2m_d}{\pi}\right)^{\frac{3}{2}} \sum_{i=1,4} \frac{A_i D_{X_i}^2}{\hbar^2 \varrho \sqrt{\Omega_i}} \frac{\vartheta(y_i)}{\exp(y_i) - 1}, \tag{5}$$

where m_d, ϱ, and A_i are the effective electron mass in bulk Ge, the crystal density, and the spin-orientation-related constants, respectively; Ω_i is the energy of the X-point zone edge phonons (X_1 and X_4). $\vartheta(y_i = \Omega_i/k_B T) = \sqrt{y_i}\exp(y_i/2)K_{-1}(y_i/2)$ is related to the modified Bessel function of the second kind. D_{X_i} is the spin-flip scattering constant, which can be determined from theoretical calculations or from experiments [41]. Using Eqs. (3), (4), and (5), we analyze the experimental data in Fig. 4, where the τ_{imp0}, Δ_{so}, D_{X_1}, and D_{X_4} are utilized as fitting parameters. For the nondegenerate Ge, we used that $m_d = 0.22 m_0$ [44], $\varrho = 5.323$ g/cm^3, $A_1 = 8$, $A_4 = 4$, $\Omega_1 = 29$ meV, and $\Omega_4 = 33$ meV [41]. From the fitting as shown in the red curve in Fig. 4, we obtain $\tau_{imp0} = 11.7$ ns, $\Delta_{so} = 0.14$ meV, $D_{X_1} = 82.0$ meV/Å, and $D_{X_4} = 86.0$ meV/Å. In this case, if the term of τ_{imp0} was not used, the fitted curve could not be obtained, indicating the validity of Eq. (4).

The value of τ_{imp0} (= 11.7 ns) is relatively long compared to that for degenerate Ge [26,27] because of the lower donor density. On the other hand, the value of Δ_{so} is almost the same as that in previous studies because this value depends only on the dopant species in Ge [26,27]. The D_{X_1} and D_{X_4} are also consistent with those in Ge [28]. To discuss these results, we consider each component in the red solid curve consisting of $\frac{1}{\tau_{imp}}$ shown in Eq. (4) and $\frac{1}{\tau_{phon}^{inter}}$ shown in Eq. (5). The blue dashed and green dashed curves in Fig. 4 represent the terms of τ_{imp} and τ_{phon}^{inter}, respectively. At temperatures less than 100 K, the τ_{phon}^{inter} term (green dashed line) rapidly increases and substantially deviates from the data. Thus, the T dependence of τ_{Ge} in this T region cannot be dominated by the phonon-induced spin relaxation in Ge. On the other hand, the τ_{imp} term (blue dashed curve) well explains the experimental data. Thus, the fitting results indicate that the monotonic increase of τ_{Ge} at

temperatures less than 50 K can be considered as T-dependent donor-induced spin relaxation, as described in $\tau_{\rm imp} \propto 1/\sqrt{T}$ with a $\tau_{\rm imp0}$ of 11.7 ns.

In previous studies on impurity-doped n-type Ge [23,28,29,39,45], there were some arguments about the spin relaxation mechanism with varying T. However, the donor-induced spin relaxation mechanism including $1/\sqrt{T}$ behavior has not been completely shown, as described in Sec. I. Because of the experimental difficulties, the spin relaxation related to nondegenerate multivalley semiconductors has so far been limited. In the present study, we investigated spin transport properties in well-controlled LSV devices with an n-type nondegenerate Ge channel. Consequently, our results clarify that the monotonic T dependence of $\tau_{\rm Ge}$ in the T range from 8 to 50 K is attributable to the T-dependent donor-induced intervalley spin-flip scattering proportional to $1/\sqrt{T}$ on the basis of the theory predicted by Song *et al.* [25]. We note that it is important for the nondegenerate Ge to partly consider the T-independent component of spin relaxation, i.e., $\tau_{\rm imp0}$, in addition to the $1/\sqrt{T}$ component. Therefore, the intervalley spin-flip scattering should be considered in nondegenerate semiconductors with a multivalley structure in their conduction band. For room-temperature operation of spin devices with nondegenerate Ge or Si, suppressing phonon- and donor-induced intervalley scattering by inducing strain and/or quantum well structure for the channel will be important [46,47].

IV. CONCLUSION

We studied the spin relaxation in an n-type nondegenerate Ge layer, moderately doped Ge (P: $\sim 10^{18}$ cm^{-3}). The obtained $\lambda_{\rm Ge}$ in the nondegenerate Ge was two to three times greater than that in degenerate Ge (P: $\sim 10^{19}$ cm^{-3}) in the temperature range from 8 to 100 K. We found that the $\tau_{\rm Ge}$ for the nondegenerate Ge is monotonically increased with decreasing T. The increase in $\tau_{\rm Ge}$ at temperatures less than 50 K was able to be interpreted in terms of the donor-driven spin relaxation mechanism including the $1/\sqrt{T}$ behavior in multivalley semiconductors, proposed by Song *et al.* [25]. We note that it was important for the $\tau_{\rm Ge}$ of the moderately doped nondegenerate Ge to partly consider the T-independent component of spin relaxation in addition to the $1/\sqrt{T}$ component.

ACKNOWLEDGMENTS

This work was partly supported by JSPS KAKENHI (Grants No. 17H06120, No. 19H05616, No. 19H02175, and No. 21H05000), JST PRESTO (Grant No. JPMJPR20BA), Iketani Science and Technology Foundation, The Murata Science Foundation, and the Spintronics Research Network of Japan (Spin-RNJ).

[1] I. Žutić, J. Fabian, and S. D. Sarma, Rev. Mod. Phys. **76**, 323 (2004).
[2] H. Dery, P. Dalal, Ł. Cywiński, and L. J. Sham, Nature (London) **447**, 573 (2007).
[3] X. Lou, C. Adelmann, S. A. Crooker, E. S. Garlid, J. Zhang, K. S. M. Reddy, S. D. Flexner, C. J. Palmstrøm, and P. A. Crowell, Nat. Phys. **3**, 197 (2007).
[4] I. Appelbaum, B. Huang, and D. J. Monsma, Nature (London) **447**, 295 (2007).
[5] R. Jansen, Nat. Mater. **11**, 400 (2012).
[6] M. I. D'yakonov and V. I. Perel', Sov. Phys. JETP **33**, 1053 (1971).
[7] J. M. Kikkawa and D. D. Awschalom, Phys. Rev. Lett. **80**, 4313 (1998).
[8] R. I. Dzhioev, K. V. Kavokin, V. L. Korenev, M. V. Lazarev, B. Ya. Meltser, M. N. Stepanova, B. P. Zakharchenya, D. Gammon, and D. S. Katzer, Phys. Rev. B **66**, 245204 (2002).
[9] D. Iizasa, A. Aoki, T. Saito, J. Nitta, G. Salis, and M. Kohda, Phys. Rev. B **103**, 024427 (2021).
[10] M. Ciorga, A. Einwanger, U. Wurstbauer, D. Schuh, W. Wegscheider, and D. Weiss, Phys. Rev. B **79**, 165321 (2009).
[11] T. A. Peterson, S. J. Patel, C. C. Geppert, K. D. Christie, A. Rath, D. Pennachio, M. E. Flatté, P. M. Voyles, C. J. Palmstrøm, and P. A. Crowell, Phys. Rev. B **94**, 235309 (2016).
[12] Y. Ebina, T. Akiho, H. Liu, M. Yamamoto, and T. Uemura, Appl. Phys. Lett. **104**, 172405 (2014).
[13] Z. Lin, D. Pan, M. Rasly, and T. Uemura, Appl. Phys. Lett. **114**, 012405 (2019).
[14] T. Suzuki, T. Sasaki, T. Oikawa, M. Shiraishi, Y. Suzuki, and K. Noguchi, Appl. Phys. Express **4**, 023003 (2011).
[15] M. Yamada, M. Tsukahara, Y. Fujita, T. Naito, S. Yamada, K. Sawano, and K. Hamaya, Appl. Phys. Express **10**, 093001 (2017).
[16] C. Zucchetti, F. Bottegoni, C. Vergnaud, F. Ciccacci, G. Isella, L. Ghirardini, M. Celebrano, F. Rortais, A. Ferrari, A. Marty, M. Finazzi, and M. Jamet, Phys. Rev. B **96**, 014403 (2017).
[17] M. Ishikawa, T. Oka, Y. Fujita, H. Sugiyama, Y. Saito, and K. Hamaya, Phys. Rev. B **95**, 115302 (2017).
[18] K. Hamaya, Y. Fujita, M. Yamada, M. Kawano, S. Yamada, and K. Sawano, J. Phys. D: Appl. Phys. **51**, 393001 (2018).
[19] C. Zucchetti, M. Bollani, G. Isella, M. Zani, M. Finazzi, and F. Bottegoni, APL Materials **7**, 101122 (2019).
[20] T. Sasaki, T. Oikawa, T. Suzuki, M. Shiraishi, Y. Suzuki, and K. Noguchi, Appl. Phys. Lett. **96**, 122101 (2010).
[21] S. Sato, M. Ichihara, M. Tanaka, and R. Nakane, Phys. Rev. B **99**, 165301 (2019).
[22] S. Lee, N. Yamashita, Y. Ando, S. Miwa, Y. Suzuki, H. Koike, and M. Shiraishi, Appl. Phys. Lett. **110**, 192401 (2017).
[23] Y. Zhou, W. Han, L.-T. Chang, F. Xiu, M. Wang, M. Oehme, I. A. Fischer, J. Schulze, R. K. Kawakami, and K. L. Wang, Phys. Rev. B **84**, 125323 (2011).
[24] J. H. Pifer, Phys. Rev. B **12**, 4391 (1975).
[25] Y. Song, O. Chalaev, and H. Dery, Phys. Rev. Lett. **113**, 167201 (2014).
[26] M. Yamada, Y. Fujita, M. Tsukahara, S. Yamada, K. Sawano, and K. Hamaya, Phys. Rev. B **95**, 161304(R) (2017).

[27] Y. Fujita, M. Yamada, S. Yamada, T. Kanashima, K. Sawano, and K. Hamaya, Phys. Rev. B **94**, 245302 (2016).
[28] Y. Fujita, M. Yamada, M. Tsukahara, T. Oka, S. Yamada, T. Kanashima, K. Sawano, and K. Hamaya, Phys. Rev. Appl. **8**, 014007 (2017).
[29] S. Dushenko, M. Koike, Y. Ando, T. Shinjo, M. Myronov, and M. Shiraishi, Phys. Rev. Lett. **114**, 196602 (2015).
[30] K. Sawano, Y. Hoshi, S. Kubo, K. Arimoto, J. Yamanaka, K. Nakagawa, K. Hamaya, M. Miyao, and Y. Shiraki, Thin Solid Films **613**, 24 (2016).
[31] S. M. Sze and J. C. Irvin, Solid-State Electronics **11**, 599 (1968).
[32] M. Yamada, K. Sawano, M. Uematsu, and K. M. Itoh, Appl. Phys. Lett. **107**, 132101 (2015).
[33] M. Yamada, F. Kuroda, M. Tsukahara, S. Yamada, T. Fukushima, K. Sawano, T. Oguchi, and K. Hamaya, NPG Asia Mater. **12**, 47 (2020).
[34] M. Johnson and R. H. Silsbee, Phys. Rev. Lett. **55**, 1790 (1985).
[35] F. J. Jedema, H. B. Heersche, A. T. Filip, J. J. A. Baselmans, and B. J. van Wees, Nature (London) **416**, 713 (2002).
[36] T. Kimura and Y. Otani, J. Phys.: Cond. Matter **19**, 165216 (2007).
[37] T. Kimura, N. Hashimoto, S. Yamada, M. Miyao, and K. Hamaya, NPG Asia Mater. **4**, e9 (2012).
[38] M. E. Flatté and J. M. Byers, Phys. Rev. Lett. **84**, 4220 (2000).
[39] K. Hamaya, Y Baba, G. Takemoto, K. Kasahara, S. Yamada, K. Sawano, and M. Miyao, J. Appl. Phys. **113**, 183713 (2013).
[40] T. Shiihara, M. Yamada, M. Honda, A. Yamada, S. Yamada, and K. Hamaya, Appl. Phys. Express **13**, 023001 (2020).
[41] P. Li, Y. Song, and H. Dery, Phys. Rev. B **86**, 085202 (2012).
[42] D. K. Wilson, Phys. Rev. **134**, A265 (1964).
[43] W. G. Spitzer, F. A. Trumbore, and R. A. Logan, J. Appl. Phys. **32**, 1822 (1961).
[44] G. Dresselhaus, A. F. Kip, and C. Kittel, Phys. Rev. **98**, 368 (1955).
[45] C. Guite and V. Venkataraman, Appl. Phys. Lett. **101**, 252404 (2012).
[46] T. Naito, M. Yamada, S. Yamada, K. Sawano, and K. Hamaya, Phys. Rev. Appl. **13**, 054025 (2020).
[47] C. Zucchetti, A. Ballabio, D. Chrastina, S. Cecchi, M. Finazzi, M. Virgilio, G. Isella, and F. Bottegoni, Phys. Rev. B **101**, 115408 (2020).